ACS OMEGA

Open Access

http://pubs.acs.org/journal/acsodf

Article

Fabrication and Properties of Adsorptive Ceramic Membrane Made from Kaolin with Addition of Dolomite for Removal of Metal Ions in a Multielement Aqueous System

Munkhpurev Bat-Amgalan, Naoki Kano,* Naoto Miyamoto, Hee-Joon Kim, and Ganchimeg Yunden

Cite This: *ACS Omega* 2024, 9, 43068−43080

Read Online

ACCESS | Metrics & More | Article Recommendations

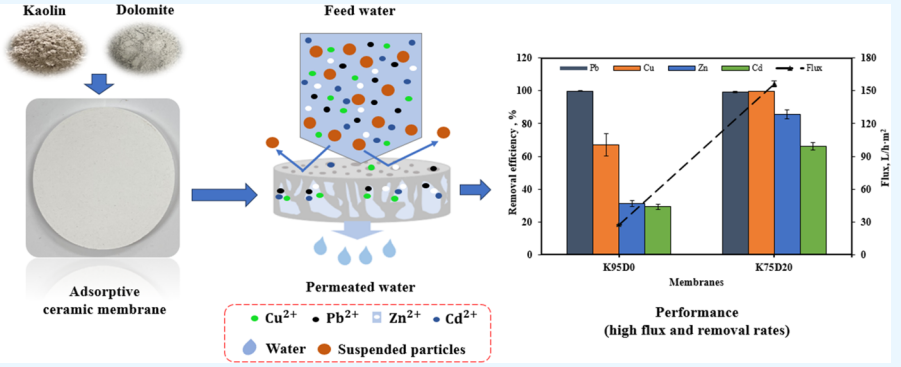

ABSTRACT: The exorbitant presence of heavy metals has emerged as one of the most serious ecological issues facing the world. The treatment processes currently employed are not effective for removing all of the contaminants completely. Therefore, it is necessary for better operational technology to be developed. Here, we fabricated effective and inexpensive kaolin-based ceramic membranes with the addition of dolomite using a simple dry compaction method. Moreover, we applied the obtained adsorptive membranes to the removal of lead, copper, zinc, and cadmium from aqueous solutions. The membranes prepared with dolomite addition (sintered at different temperatures) exhibited a high water flux between 246.78 and 1738.56 L/h·m^2 at an extremely low operating pressure (0.03 MPa). Furthermore, the optimal membrane showed high removal efficiencies of 99.12, 99.82, 85.62, and 65.94% for Pb(II), Cu(II), Zn(II), and Cd(II), respectively. The utilization of dolomite enhanced the removal efficiency of the adsorptive membranes by around 32−54% in a multielement system. This work reveals that enhanced adsorptive membranes with high fluxes and strong removal abilities have great potential as a synergized system with practical applications in the removal of heavy-metal contaminants from wastewater in the future.

INTRODUCTION

Clean water is a crucial substance that ensures the survival of all living things and protects nature on Earth. Nonetheless, the most pressing problems humans currently face can be related to water pollution by various types of contaminants from human activities, which leads to a shortage of drinkable water. Namely, heavy-metal ions [Pb(II), Cu(II), Cd(II), Zn(II), Co(II), and Ni(II)] existing in water bodies are raising concerns because of their highly deleterious and nonbiodegradable effects on human health and the environment.[1−3] Heavy metals are mainly released into water streams from various industries including the microelectronics, battery, electroplating, mining, tannery, agricultural, and chemical industries.[4,5] To date, technologies such as ion exchange, coagulation, chemical precipitation, adsorption, electrodialysis, and membrane filtration have been designed for removing heavy metals from water.[6,7] Among them, adsorption is considered the most effective process for the removal of heavy metals, providing a simple design and operation.[2,8] However, commercial adsorbents are expensive and still face some drawbacks, such as the resistance of internal diffusion and their sluggish performance. Therefore, there is an urgent need to develop and find more effective technologies for wastewater treatment to remove heavy-metal ions. As a promising alternative, adsorption combined with ceramic membrane technology has an excellent ability to remove heavy metals, and both adsorption and filtration can be performed in a single step.[9,10]

Received: July 23, 2024
Revised: September 25, 2024
Accepted: September 30, 2024
Published: October 10, 2024

Ceramic membranes have desirable properties, in terms of their chemical and thermal stability and mechanical strength. These excellent characteristics offer advantages such as long lifetimes and the ability to withstand extreme temperatures and pH values in many applications.[11] Despite all of these advantages, inorganic membrane products require high-cost materials (alumina, silica, zirconia, and titania) and high sintering temperatures, limiting their application on a large scale.[12] To resolve these shortcomings, recent studies on the preparation of ceramic membranes have employed inexpensive materials such as dolomite,[13] clay,[14] kaolin,[15,16] fly ash,[17] zeolite,[9] bentonite,[18] and apatite[19] to reduce the high costs and firing temperatures. Kaolin is a type of soft clay and an alternative raw material for membrane fabrication that exhibits distinctive properties including its low plasticity, high temperature resistance, stable pore size formation, cost-effectiveness, and hydrophilicity.[20,21] These membranes' hydrophilic properties, as well as the active groups they contain, allow them to interact with heavy-metal ions.[1] In addition, dolomite is a natural mineral that consists of magnesium and calcium double carbonate. It plays a vital role as a pore former in membrane technology and as an adsorbent with a strong ability to remove heavy-metal ions from water sources.[22−24] The fundamental physicochemical properties of kaolin and dolomite used for ceramic membrane preparation make them ideal for use as adsorptive ceramic membranes. The main adsorption process for removing heavy metals involves the mechanism of chemical and physical interaction between the membrane sides and metal ions in the feed stream.[25] There have been combined membrane studies and experiments on heavy-metal removal. For example, Foorginezhad et al.[1] synthesized a composite adsorptive ceramic membrane (tubular) from SnO_2 and montmorillonite for the removal of Cu(II), Zn(II), and Ni(II). The membrane was noted to possess 99.26% Cu(II), 92.23% Zn(II), and 64.74% Ni(II). Many other studies fabricated and developed adsorptive membranes based on copper, graphene oxides (nanoparticles), metal−organic frameworks, carbon nanotubes, and zeolite combined with different clays, zirconia, alumina, or clay−alumina supports for Cr(VI), Cr(III), Cu(II), Ni(II), Pb(II), Co(II), Hg(II), Zn(II), and Cd(II) removal.[4,9,26−31] The addition of oxide materials with specific adsorption capabilities in combined membranes provides great potential for enhancing the removal performance. On the other hand, the choice of raw materials and their appropriate combination are very important in the field of adsorptive membrane fabrication. The production method of nanomaterials such as metal−organic frameworks and carbon nanotubes (which require several syntheses) is not simple. This type of membrane can work in the range of nanofiltration. High-pressure-driven membranes require high operating pressure, resulting in low permeate and high energy use.[32,33]

In fact, relatively few studies have reported adsorptive membranes made from different materials or combinations (e.g., dolomite and kaolin) for the various heavy metals in multimetal systems. As a further contribution, a great number of studies are still needed in order to gain a better understanding of this combined technology as well as adsorptive membranes.

Based on the above considerations, here, we designed ceramic membranes based on kaolin and dolomite. Dolomite plays the roles of both the main adsorbent and the pore former. Therefore, the first objective of this study is to evaluate the effect of dolomite addition on the structure and properties of the porous ceramic membranes. Also, the influence of the sintering temperature and time on the membranes with optimal compositions was studied based on their characteristics such as their mechanical strength and pure water flux. The second aim is to assess the removal of lead, copper, zinc, and cadmium using the selected membranes in a multimetal solution with the designed single-batch system. This work highlights some novel findings as follows: (a) the cheap starting materials, such as kaolin and dolomite, and the low sintering temperature enable the low-cost production of membranes; and (b) dolomite combined with kaolin plays a significant role in membrane preparation, possessing promising performance in the removal of heavy metals and a high flux at low applied pressures.

MATERIALS AND METHODS

Materials. Dolomite and kaolin were provided by Ueda Lime Manufacturing Co., Ltd. and Kusaba Chemical Co., Ltd. (Gifu, Japan), respectively. Methylcellulose with a viscosity of 4000 cP, standard solutions of metal ions (Pb^{2+}, Cu^{2+}, Zn^{2+}, and Cd^{2+}) with a concentration of around 1000 mg/L, and element nitrate salts including $Pb(NO_3)_2$, $Cu(NO_3)_2{\cdot}3H_2O$, $Zn(NO_3)_2{\cdot}6H_2O$, and $Cd(NO_3)_2{\cdot}4H_2O$ with a purity of 98.0−99.5% were supplied by Kanto Chemical Co., Inc. (Tokyo, Japan). As received, other chemical reagents were of analytical grade, and all of the chemicals were used without further purification. Throughout the experimental process, deionized water (>18.2 MΩ) obtained from an ultrapure water instrument (RFU 424TC, Advantec, Toyo Seisakusho Kaisha., Ltd., Japan) was used.

Membrane Preparation. Ceramic membranes (dry basis) were fabricated from kaolin, dolomite, and methylcellulose according to the mass ratios shown in Table 1. First, kaolin and dolomite were uniformly mixed with 5 wt % of an organic binder, namely, methylcellulose, and pressed at a pressure of 300 kgf/cm^2 in a cylinder mold (diameter of 40 mm and thickness of 3 mm). This step was followed by a sintering process to obtain the final ceramic membranes at varying temperatures (950−1250 °C) and times (1−5 h) using an electric furnace (NHK-170, Nitto Kagaku Co., Ltd.). The sintering temperature was gradually increased to 250 °C and held for 1 h to evaporate residual water. Then, heating at 450 °C was employed to remove the organic binder. The temperature and time were further increased to different desired values (950−1250 °C and 1−5 h, respectively) to determine the optimal sintering temperature and time. Eventually, the sintered membranes were cooled to reach the ambient temperature. A series of ceramic membranes containing kaolin and dolomite were labeled, as shown in Table 1.

Table 1. Compositions of Materials Used in Membrane Fabrication

	wt %	
membrane names	kaolin	dolomite
K95D0	95	0
K85D10	85	10
K80D15	80	15
K75D20	75	20
K70D25	70	25
K65D30	65	30

For the mechanical strength measurement, ceramic cube-shaped bodies (wet basis) were prepared. The materials (as shown in Table 1) were accurately weighed and mixed with 40

https://doi.org/10.1021/acsomega.4c06785
ACS Omega 2024, 9, 43068−43080

wt % distilled water. The ceramic bodies were printed using a cube mold (2 × 2 cm) and dried at 110 °C for 24 h; then, they were subjected to the sintering conditions described above.

Characterization. The elemental compositions of the raw starting materials kaolin and dolomite were determined by using the X-ray fluorescence technique (SEA1200VX, SII Vortex, Akishima, Tokyo, Japan). The thermal and mass changes in the raw starting materials and powders mixed with different compositions were studied via thermogravimetric analysis (TGA) and differential thermal analysis (DTA) (ThermoPlus2 TG8120, RIGAKU, Tokyo, Japan). The mineral compositions of the materials and membranes were detected via XRD (D2 Phaser, Bruker, Billerica, MA). A scanning electron microscope (SEM, JCM-6000, JEOL Tokyo, Japan) was used to observe the morphology and microstructure of the membranes. The particle size distributions of the powders were obtained based on analysis of the SEM images using ImageJ software. The X-ray photoelectron spectroscopy (XPS, K-Alpha, Thermo Scientific Center, Waltham, MA) measurement was also carried out to confirm the adsorption mechanisms. The surface texturing properties (membranes), namely, surface area, pore volume, and pore size, were identified using Brunauer−Emmet−Teller apparatus (TriStar II 3020, Micromeritics, Norcross, GA), and before analysis, samples were pretreated at 423 K for 2 h.

Water absorption was determined by the difference in weight between the dried and the immersed membranes. The membrane bodies were soaked in distilled water for around 24 h in accordance with Archimedes' principle. Water absorption was determined using the formula

$$\text{water absorption } (\%) = \frac{m_0 - m_1}{m_1} \times 100 \quad (1)$$

where m_0 and m_1 are the weights of the wet and dry membranes, respectively.

The measurement of the mechanical strength was made by applying pressure until the membrane samples (cube-shaped) broke. The mechanical strength (R, MPa) was evaluated using the equation

$$R = F/S \quad (2)$$

where F is the maximum force on the membrane (Newton) and S is the active membrane area (mm^2).

Lab-scale cross-flow filtration set to 0.03 MPa pressure and room temperature was used to test the water flux. The pure water flux, J ($L/h{\cdot}m^2$), was calculated by collecting the filtered water volume through the membrane pores in unit time as defined in the following equation:

$$J = \frac{V}{A \times \Delta t} \quad (3)$$

where V is the total volume of water after filtration (L), Δt is the measured time (h), and A is the valid membrane area (m^2).

The volume (V_m, cm^3) and density (ρ_m, g/cm^3) of the ceramic membranes sintered at different temperatures were calculated by the following equations:

$$V_m = \frac{d^2 \pi h}{4} \quad (4)$$

$$\rho_m = \frac{m_m}{V_m} \quad (5)$$

where d is the diameter of the membrane (cm^2), h is the thickness of the membrane (cm), and m_m is the dried membrane mass (g).

Performance of Membranes in Removal of Complex Metal Ions. We conducted experiments for the removal of multiple metal ions using the obtained ceramic membranes in lab-scale cross-flow filtration mode (as shown in Figure 1). The

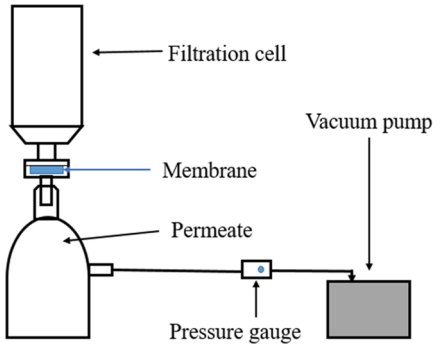

Figure 1. Schematic diagram of the dead-end cell.

ceramic membranes are disk-shaped with a membrane area of approximately 0.855×10^{-3} m^2. The ceramic membrane was placed in a dead-end filtration setup (Figure 1) and then applied for the removal of multiple metal ions. The experiments using the five different membranes were carried out at room temperature and pH 5 with an applied pressure of 0.015 MPa. Three solutions with different concentrations of 10, 50, and 100 mg/L served as the feed solutions. The filtration amount of one time is 50 mL. The adsorption amount of metal ions in the filtrate was calculated from the concentration determined by inductively coupled plasma atomic emission spectrometry (SPS1500 V, Seiko, Chiba, Japan). The permeate flux was also calculated. The removal performance (R, %) was determined using the equation

$$R\ (\%) = \frac{C_f - C_p}{C_f} \times 100 \quad (6)$$

where C_f is the amount of metal ions before filtration (mg/L) and C_p is the amount of metal ions after filtration (mg/L).

Moreover, the most effective parameters for membrane fabrication are sintering temperature and time. Therefore, the appropriate sintering temperature and time were considered based on the membrane characteristics such as their mechanical strength, pure water flux, and removal rate.

In this article, all of the experiments were performed more than three times. Then, the error bars were drawn based on the calculation of standard deviation.

RESULTS AND DISCUSSION

Characterization of Raw Materials. The elemental compositions of kaolin[34] and dolomite are listed in Table 2. It is noted that the main elements of kaolin are 54.12 wt % Si and 38.92 wt % Al, which are widely employed raw materials in the preparation of ceramic membranes.[34] The major elements of dolomite are 74.05 wt % Ca and 21.09 wt % Mg, so it theoretically contains both calcium and magnesium carbonates. Also, CO_2 is released during the thermal decomposition of these carbonates, suggesting the potential to produce membranes with a porous structure.

https://doi.org/10.1021/acsomega.4c06785
ACS Omega 2024, 9, 43068−43080

Table 2. Elemental Analysis (XRF) of Kaolin and Dolomite

	wt %	
elements	kaolin	dolomite
Si	54.12	2.78
Al	38.92	0.66
Ca	0.27	74.05
K	3.94	0.41
Mg	2.28	21.09
Fe	0.47	0.61
Mn		0.33
others		0.07

The SEM images and particle size distributions of the kaolin and dolomite powders are listed in Figure 2a–d. The morphology of kaolin (a) displayed uniform particles with different shapes, but dolomite (c) showed irregularly sized particles (big and small particles) with various chunks. Also, the average particle size of both kaolin (b) and dolomite (d) predominated in the small range below around 15 μm.

Figure 3 shows the XRD results of the raw kaolin[34] and dolomite powders. Based on Figure 3, the main crystalline phases in the kaolin powder are kaolinite, Illite, and quartz. The significant intense peaks at 12.33° and 24.82° (2θ) indicate the presence of the kaolinite phase.[34] The major phases present in the dolomite powder are dolomite and calcite. The high peak observed at a 2θ of 30.96° corresponds to the dolomite phase.

The TG and DTA results of the kaolin, dolomite, and methylcellulose powders are shown in Figure 4A–C. From the TG curves (solid black lines in Figure 4A–C), the total weight losses of kaolin, dolomite, and methylcellulose were 17.22, 42.5, and 96.9%, respectively. In the DTA analysis of kaolin (solid red line in Figure 4A), the three peaks noted were exothermic and endothermic peaks. Weak and sharp endothermic peaks appeared at 561.4 and 659.7 °C, corresponding to the dehydroxylation, which refers to kaolin shifting into metakaolin. The sharp exothermic peak noted at 1009.8 °C indicates the crystallization of the primary mullite. In the DTA results for dolomite (Figure 4B), one endothermic peak at 735.6 °C can be observed, which is related to the decomposition of dolomite ($CaMg(CO_3)_2$) into MgO and CaO, releasing CO_2. In the DTA line for methylcellulose (Figure 4C), three exothermic peaks at 317.7, 387.6, and 480.1 °C can be observed, which correspond

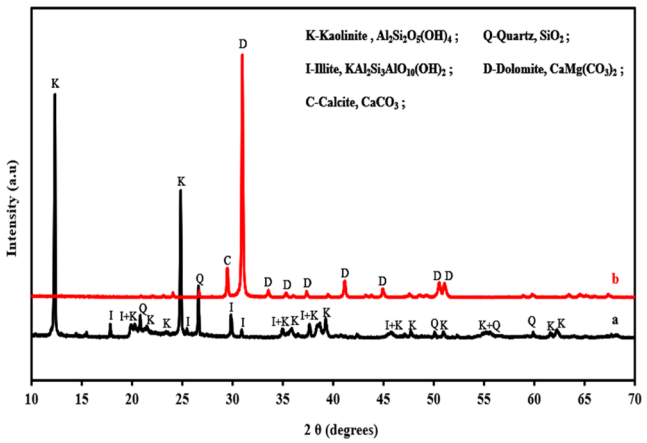

Figure 3. XRD patterns of kaolin (a) and dolomite (b).

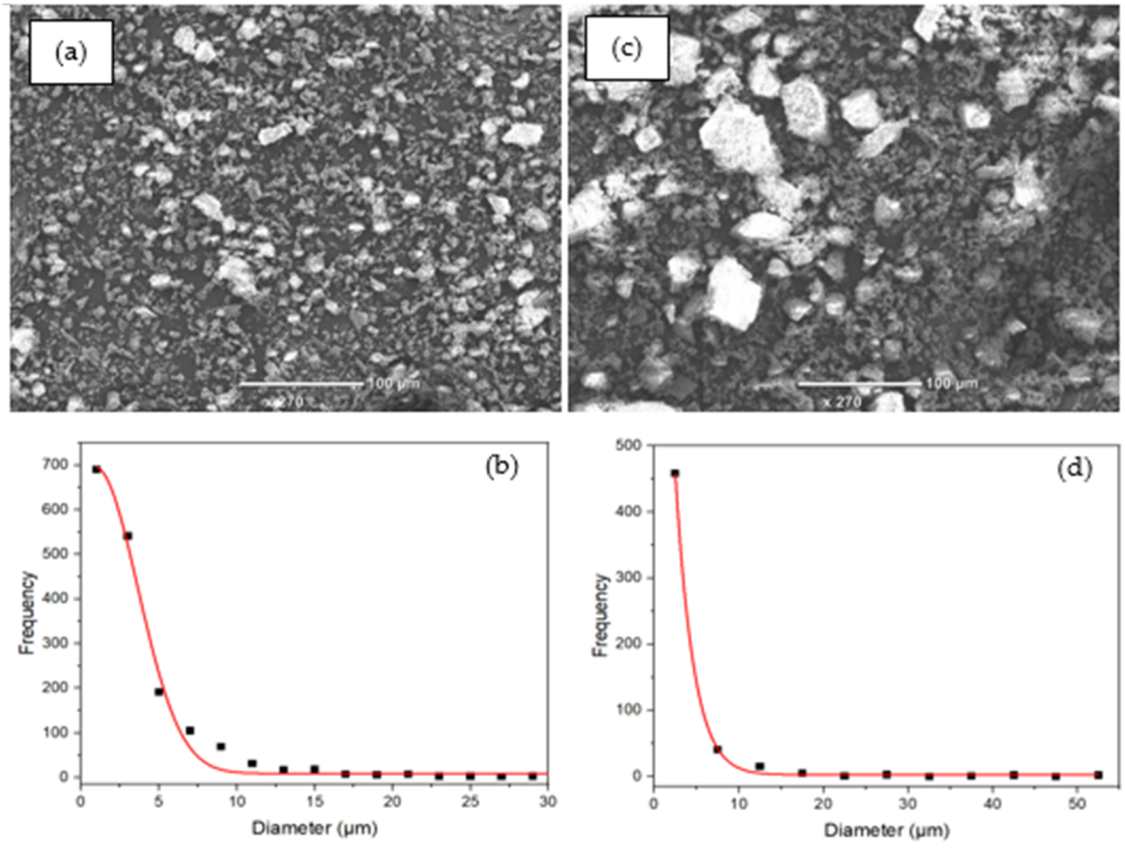

Figure 2. SEM images and particle size distribution of the kaolin (a, b) and dolomite (c, d) powders.

https://doi.org/10.1021/acsomega.4c06785
ACS Omega 2024, 9, 43068−43080

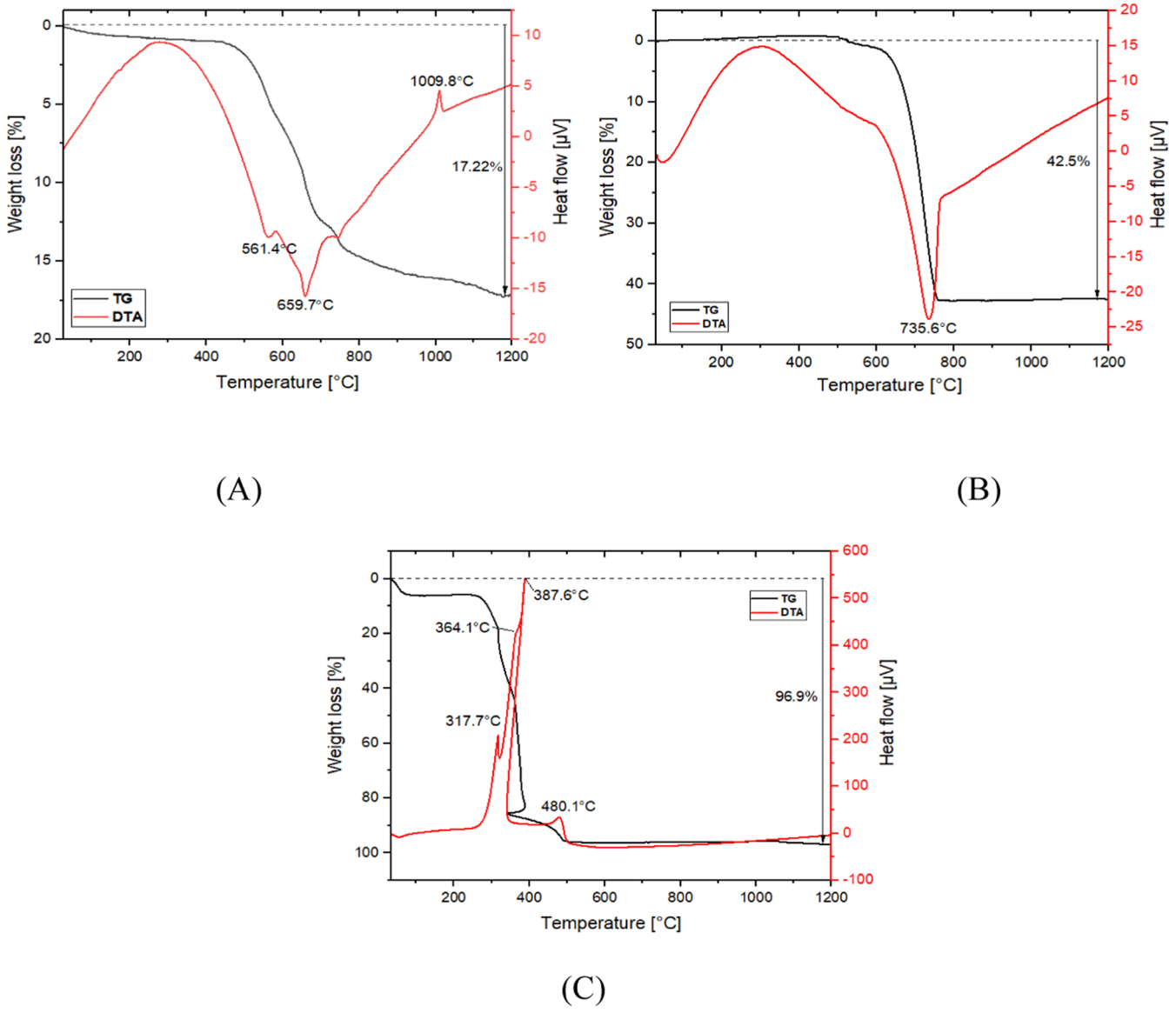

Figure 4. Thermogravimetric-differential thermal analysis (TG−DTA) curves for kaolin (A), dolomite (B), and methylcellulose (C).

to methylcellulose being entirely burned from the membrane during the sintering process.

Characterization of the Ceramic Membranes. The compared weight loss (TG) results of the ceramic membranes produced with and without different dolomite additions (0−30%) are presented in Figure 5. The total weight losses of the membranes were between 17.34 and 27.20%. With the increase in the weight percent of dolomite from 10 to 30, the total weight loss increased notably. The total weight loss for K95D0 (without dolomite addition) was much lower than that of K65D30 (dolomite addition of 30 wt %), and this observation indicates that the dolomite addition has a significant effect on the membrane properties. Also, the TG and DTA curves of the optimal mixed sample containing 20 wt % dolomite are shown in Figure 6. In the TG curves, significant weight losses can be observed in several regions. In the range 300−400 °C, the weight loss is attributed to the burning process of methylcellulose, which is related to the exothermic peak at 326.5 °C in the DTA curve. Further weight losses occurred between 500 and 800 °C due to the phase transition of kaolin to metakaolin and the decomposition of dolomite. These observations are

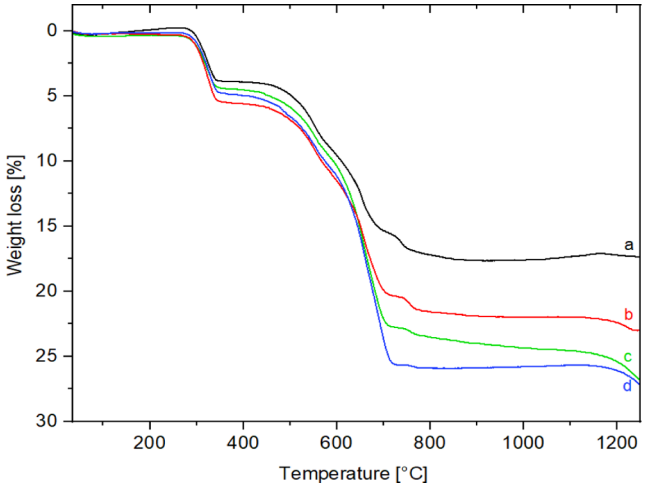

Figure 5. TG curves for the powders mixed in different compositions (a-K95D0, b-K85D10, c-K75D20, and d-K65D30).

https://doi.org/10.1021/acsomega.4c06785
ACS Omega 2024, 9, 43068−43080

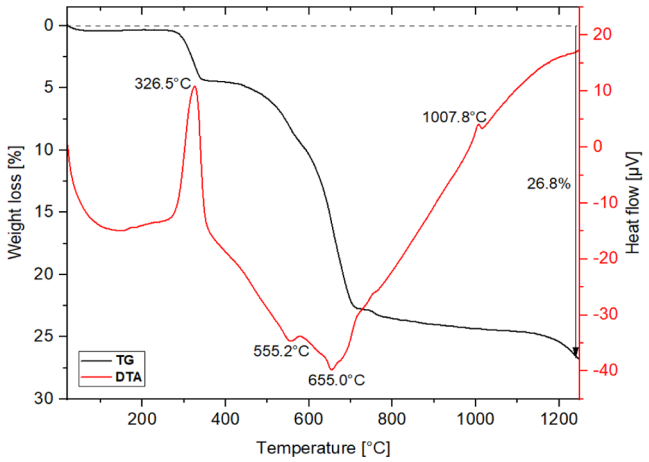

Figure 6. TG−DTA curves for the mixed powder (K75D20).

confirmed by the endothermic peaks at 555.2 and 655.0 °C in the DTA analysis, respectively. Finally, the weight loss appearing in the range of 1150−1250 °C may be explained by the formation of cordierite and anorthite phases.

The XRD patterns of the K75D20 ceramic membrane sintered at different temperatures for 4 h are shown in Figure 7. The ceramic membranes sintered at a temperature of 1150 °C

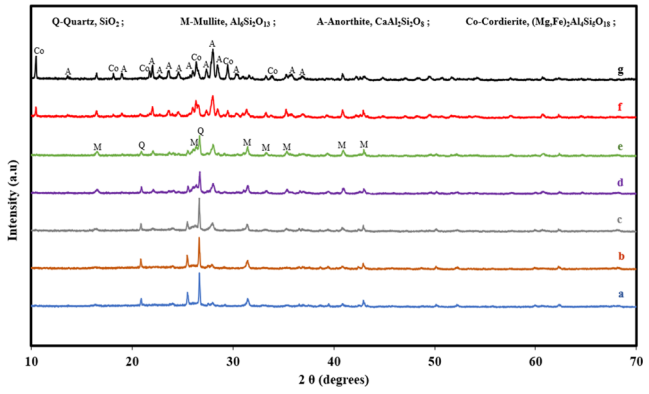

Figure 7. XRD patterns of K75D20 membranes sintered at 950 °C (a), 1000 °C (b), 1050 °C (c), 1100 °C (d), 1150 °C (e), 1200 °C (f), and 1250 °C (g) for 4 h.

or lower mainly contained mullite, quartz, and a certain amount of anorthite phases. With the increase in the sintering temperature from 950 to 1150 °C, the intensities of mullite and anorthite increased, while the intensities of quartz decreased. These observations indicate that mullite formed through the transformation of metakaolin, and anorthite appeared due to the interaction of CaO (decomposition of $CaCO_3$ in dolomite) with the alumina and silica structure in kaolin. For the membranes sintered at temperatures greater than 1150 °C (at 1200−1250 °C), the quartz peaks disappeared, a small amount of mullite was left, and anorthite and cordierite minerals predominated. The cordierite and anorthite minerals formed from mullite with the increase in the sintering temperature; the related formulas are presented below (eqs 7 and 8).[11] It is worth noting that the theoretical eutectic temperatures of anorthite and cordierite (CaO-SiO_2−Al_2O_3 and MgO-SiO_2−Al_2O_3 systems) are around 1170[24] and 1365 °C,[20] respectively.

$$[Al_2O_3{\cdot}2SiO_2](\text{mullite}) + 3CaO + 4SiO_2 \rightarrow 3[CaO{\cdot}Al_2O_3{\cdot}2SiO_2](\text{anorthite}) \quad (7)$$

$$2[3Al_2O_3{\cdot}2SiO_2](\text{mullite}) + 6MgO + 11SiO_2 \rightarrow 3[2MgO{\cdot}2Al_2O_3{\cdot}5SiO_2](\text{cordierite}) \quad (8)$$

The SEM images of the K75D20 membranes sintered at 1100, 1150, 1200, and 1250 °C for 4 h are illustrated in Figure 8a−d. As can be seen in Figure 8a−d, similar microstructures and pores were observed in the K75D20 membranes sintered at 1100 and 1150 °C. However, with the increase in the sintering temperature to 1200 °C, broad necks and integrated pores (coalescence phenomenon) were observed on the membrane surface. In particular, this observation (broad necks and integrated pores) was recorded for the membrane sintered at 1250 °C, which may be due to the several phase transformations during sintering at a high temperature.[35] It is revealed that the membrane morphology and pore size significantly depend on the sintering temperature. The SEM results of the K75D20 membrane are compared with those of the K95D0 membrane, both sintered at the same temperature, as shown in Figure 9. It can be clearly seen that K95D0 displayed a few and smaller pores, but after the dolomite addition, the K75D20 membrane showed many large pores. This outcome reveals that the formation of a large pore structure was due to the strong phase inversion caused by the dolomite addition.

Effect of Dolomite Content on Membrane Properties. To evaluate the appropriate dolomite content, water flux and compressive strength tests were conducted by using ceramic membranes produced with and without different amounts of dolomite addition. The results are displayed in Figure 10. With the dolomite addition of 0−10%, the water flux increased sharply from 49.99 to 152.05 L/h·m^2 (three times), which continued until the addition of 20% dolomite and increased gradually with the addition of 30% dolomite. These water flux results suggest that dolomite is a good pore former for ceramic membranes. The compressive strength increased with the increase in the dolomite amount from 0 to 20% (0.81−1.1 MPa) and then dropped from 1.1 MPa to 0.92 with the further addition of dolomite (from 20 to 30%). From these observations, dolomite may improve the mechanical strength of the membrane in the dolomite amount from 0 to 20%, but the further enhancement of the dolomite content degrades the membrane due to the formation of a large pore structure, which leads to a decrease in the physical strength of the membrane.[22] In addition, the difference (from 0.81 to 1.1 MPa) in the mechanical strength of the ceramic membranes (K95D0−K65D30) prepared with different additions was small. The membranes were sintered at low temperatures. Therefore, the main phases did not completely form in the membrane body, which resulted in a small difference in the strength of the membranes. On the other hand, the membranes showed a high water flux, even a low operating pressure (0.03 MPa). Therefore, it can be considered that the appropriate dolomite addition is 20 wt %.

Effect of Sintering Time on Membrane Properties. To investigate the appropriate sintering time, water flux and compressive strength experiments were carried out on the K75D20 membrane with sintering times of 1−5 h. The obtained results are listed in Figure 11. The mechanical strength (1.1−1.37 MPa) was gradually enhanced with an increase in the sintering time from 1 to 5 h. This increase suggests that the particles of the materials become better connected with

https://doi.org/10.1021/acsomega.4c06785
ACS Omega 2024, 9, 43068−43080

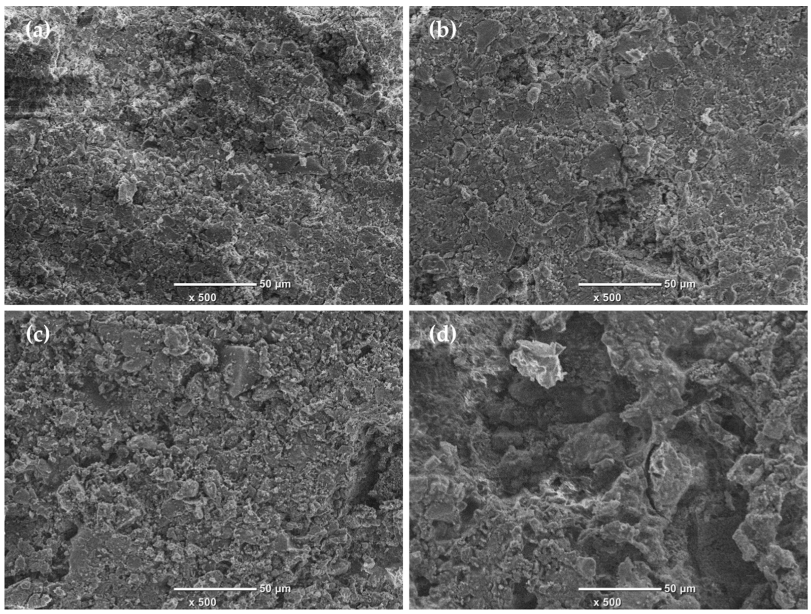

Figure 8. SEM images of K75D20 membranes sintered at 1100 °C (a), 1150 °C (b), 1200 °C (c), and 1250 °C (d) for 4 h (500× magnifications).

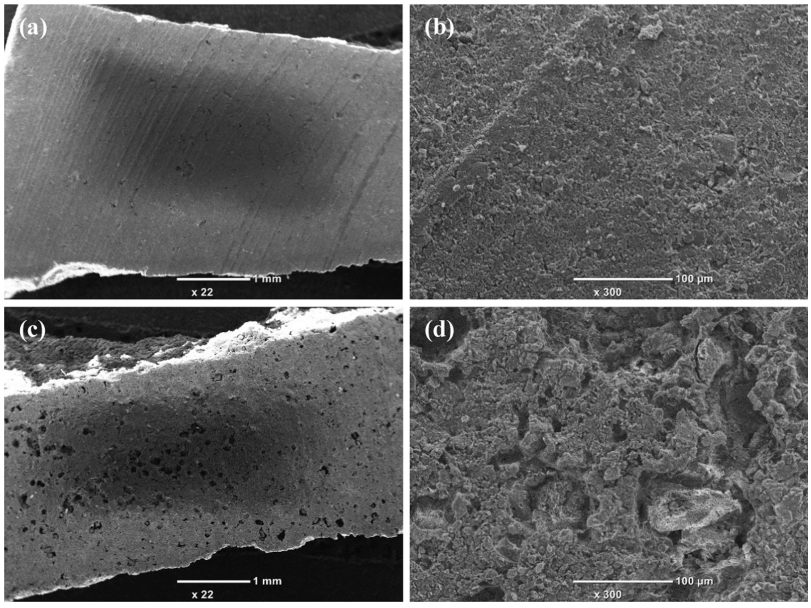

Figure 9. SEM images of K95D0 (a, b) and K75D20 (c, d) membranes sintered at 1250 °C for 4 h (22 and 300× magnifications, respectively).

increasing time, which improves the mechanical strength of the membrane. Regarding the water flux results, with the increase in the sintering time from 1 to 4 h, the water flux increased, but then it decreased at a sintering time of 5 h. These flux results indicate that the pore diameters of the membranes gradually grow with the increase in the sintering time up to a certain point; then, the opposite occurs in the form of pore shrinkage or densification, which leads to a decrease in the flux.

Effect of Sintering Temperature on Membrane Properties. To evaluate the effect of the sintering temperature, K75D20 membranes sintered at different temperatures (950 and 1250 °C) were further tested in terms of water flux and compressive strength. As shown in Figure 12, both parameters, namely, water flux and compressive strength, increased with the increase in the sintering temperature from 950 to 1250 °C. In particular, sharp increments were observed at higher temperatures of 1200−1250 °C. The mechanical strength may be controlled by several factors. The K75D20 membranes sintered at different temperatures exhibited compressive strengths of 1.09−16.69 MPa. The K75D20 membrane sintered at 1250 °C showed the highest mechanical strength, 16.69 MPa. This can be explained by the fact that the addition of dolomite, which initiates liquid phase formation during sintering and provides a stronger intermolecular interaction between the ceramic particles (kaolin and dolomite), leads to an enhancement of the membrane's mechanical strength.[17] In addition, another explanation is that the mechanism of the neck grain growth and mechanical bond formation of cordierite and anorthite by the mullite phase at a high sintering temperature improves the compressive strength. This result is confirmed by the results of the XRD patterns (Figure 7), and these good trends are consistent with the literature.[17,24] Regarding the water flux

https://doi.org/10.1021/acsomega.4c06785
ACS Omega 2024, 9, 43068−43080

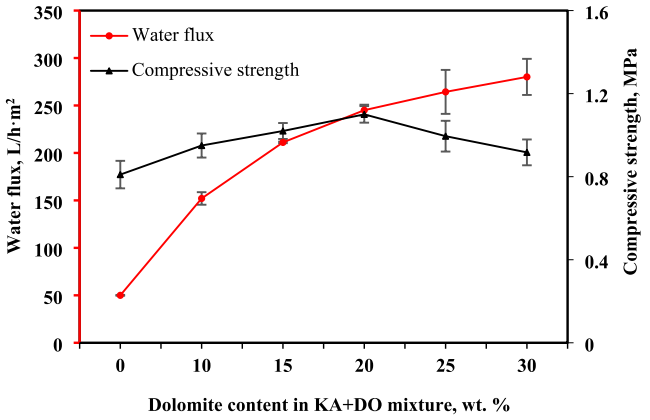

Figure 10. Effect of the dolomite content on the water flux and compressive strength of ceramic membranes based on kaolin and dolomite (sintering temperature, 1000 °C; sintering time, 1 h).

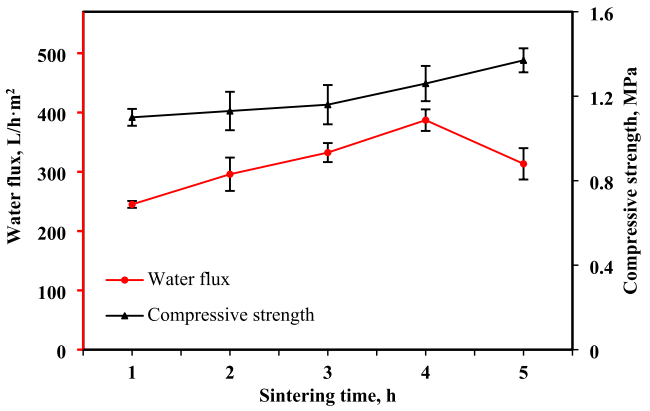

Figure 11. Effect of sintering time on water flux and compressive strength of K75D20 membranes (sintering temperature, 1000 °C).

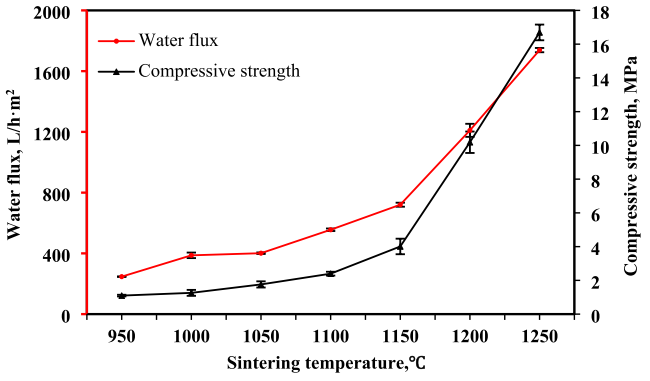

Figure 12. Effect of the sintering temperature on the water flux and compressive strength of K75D20 membranes (sintering time, 4 h).

results, the K75D20 membranes showed water fluxes of 246.78–1738.56 L/h·m^2 with the increase in the sintering temperature. In particular, the water flux of the membrane sintered at 1250 °C rapidly increased (from 1.4 to 7 times) to 1738.56 L/h·m^2 compared to that of the K75D20 membranes sintered at lower temperatures. However, the increase in the sintering temperature mostly led to an increase in the density, grain growth, and shrinkage of the membranes. Notably, this phenomenon occurs rapidly at high operating temperatures, in turn reducing the porosity and permeability. However, in our case, the water flux did not show a declining trend with increasing temperatures. The possible reason for this observation could be explained by the slow decomposition of dolomite. The dolomite addition minimized the shrinkage and density of the membrane, which prevented a decrease in the water flux. Magnesium carbonate has several main advantages such as higher porosity, moderate pore size, and low shrinkage. In addition, both the water flux and mechanical strength were improved with increasing sintering temperatures from 950 to 1250 °C.

The results of the mean pore sizes and water absorption on the K75D20 membranes sintered at different temperatures are illustrated in Figure 13 and Table 3. The increase in the sintering

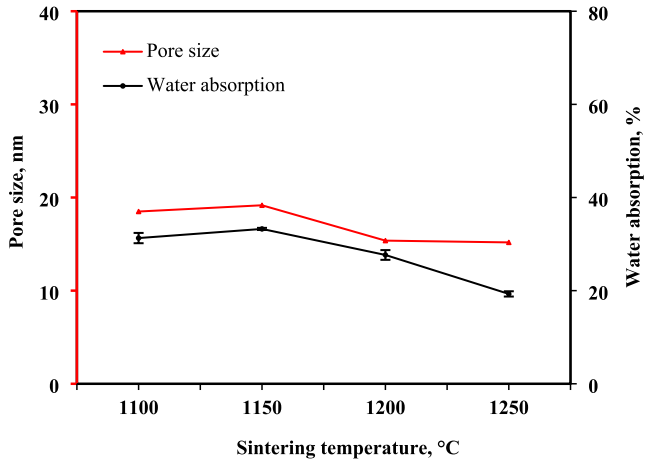

Figure 13. Results of the mean pore sizes by Brunauer–Emmett–Teller (BET) analysis and water absorption on the K75D20 membranes sintered at 1100, 1150, 1200, and 1250 °C for 4 h.

Table 3. BET Surface Area, Pore Size, and Pore Volume of Ceramic Membranes Sintered at Different Temperatures for 4 h

sample	BET surface area ($m^2 \cdot g^{-1}$)	pore volume ($cm^3 \cdot g^{-1}$)	pore size (nm)
1100 °C	2.9394	0.013591	18.49497
1150 °C	2.5847	0.012385	19.16647
1200 °C	0.9630	0.003700	15.37066
1250 °C	0.5005	0.001899	15.17969

temperature from 1100 to 1250 °C led to a decrease in the average pore size from 18 to 15 nm, while water absorption decreased from 31.29 to 19.29%. The observation of decreased average pore sizes suggests that pore shrinking is caused by an increase in the sintering temperature. Therefore, the K75D20 membranes sintered at high temperatures have a small pore size, which led to a decrease in the water absorption amount.

Also, the density of the ceramic membranes sintered at different temperatures is changed from 1.4 to 1.5 g/cm^3. The results are shown in Figure 14. From the result, the density increased with the increase in the sintering temperature because of the pore shrinking.

Membrane Performance and Mechanism for the Removal of Complex Heavy Metals. First, the K95D0 and K75D20 membranes produced with different compositions (same sintering temperature and time) were tested with 10 mg/L multielement (Pb^{2+}, Cu^{2+}, Zn^{2+}, and Cd^{2+}) solution. As shown in Figure 15, the K95D0 membrane exhibited removal rates of 99.83% Pb(II), 67.20% Cu(II), 31.27% Zn(II), and 29.37% Cd(II). These considerable removal rates can be explained by

https://doi.org/10.1021/acsomega.4c06785
ACS Omega 2024, 9, 43068–43080

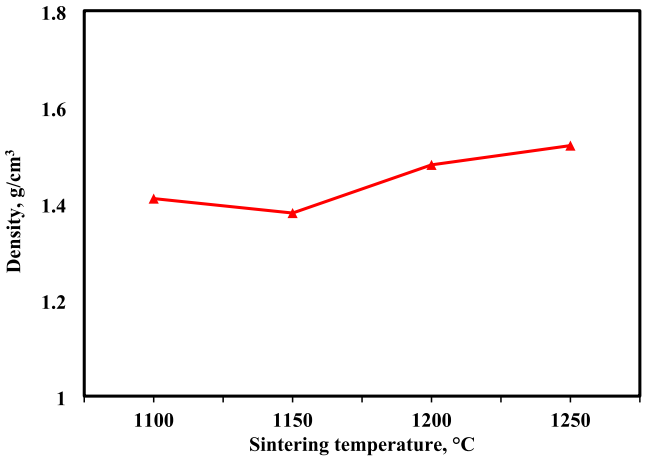

Figure 14. Density of the K75D20 membranes sintered at 1100, 1150, 1200, and 1250 °C for 4 h.

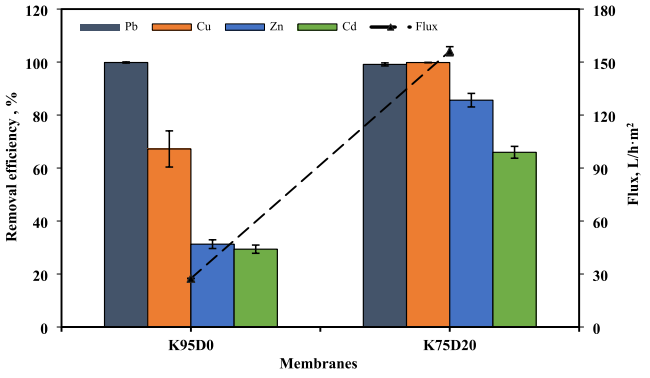

Figure 15. Complex heavy-metal removal efficiency and flux of the K95D0 and K75D20 membranes sintered at 1100 °C for 4 h (applied pressure, 0.015 MPa; pH 5; feed concentration of complex metals, 10 ppm).

the interaction of the functional groups (active sites) on the pore walls of the K95D0 membrane.[1] In addition, the K75D20 membrane showed removal rates of 99.12% Pb(II), 99.82% Cu(II), 85.62% Zn(II), and 65.94% Cd(II), which, except for Pb(II), were approximately 1.5 (Cu(II)), 2.7 (Zn(II)), and 2.2 (Cd(II)) times higher than those of a pristine K95D0 membrane, respectively. The presence of dolomite addition supplies greater amounts of calcium and magnesium to the membrane. During the sintering process, calcium and magnesium elements can bond to aluminosilicates via a weak electrostatic interaction. Therefore, this allows for ion exchanges between heavy-metal ions in feed solutions with an acidic pH and exchangeable cations such as Ca^{2+}, Mg^{2+}, and K^{2+} or charged H^+ ions on the membrane surface and inner side. The ion exchange mechanism is as follows (eq 9):[9,36]

$$[M^{-}A^{+}] + Cation^{+} \leftrightarrow [M^{-}Cation^{+}] + A^{+} \quad (9)$$

In addition, the permeate flux of the K75D20 membrane (156.2 L/h·m^2) for metal ions was about 5.7 times higher than that of the K95D0 membrane (27.5 L/h·m^2). These results show that the addition of dolomite enhanced both the removal rate and permeate flux.

The K75D20 membranes sintered at different temperatures were also applied to the removal of heavy metals and permeate flux. As shown in Figure 16 and Table 4, the removal rates of the membranes for heavy metals decreased noticeably when the

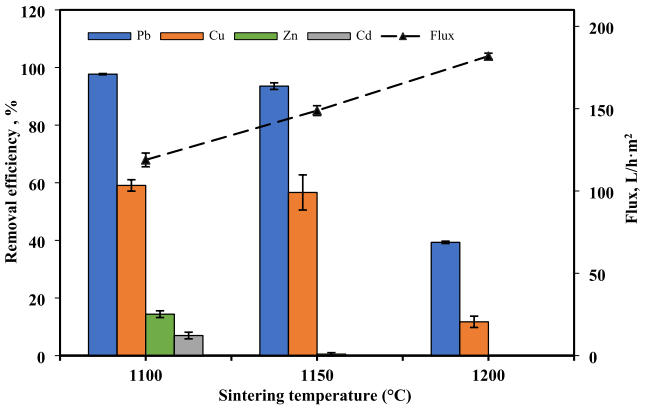

Figure 16. Complex heavy-metal removal efficiency and flux of the K75D20 membranes sintered at different temperatures for 4 h (applied pressure, 0.015 MPa; pH 5; feed concentration of complex metals, 50 ppm).

Table 4. Complex Heavy-Metal Removal Efficiency and Flux of the K75D20 Membranes Sintered at Different Temperatures for 4 h[a]

sintering temperature (°C)	flux (L/h·m^2)	removal rate (%)			
		Pb	Cu	Zn	Cd
1100	118.8906	97.69	59.07	14.38	6.97
1150	148.824	93.54	56.63	0.53	0.00
1200	181.9229	39.32	11.73	0.00	0.00
1250	690.7532	0.00	3.30	0.00	0.00

[a]Applied pressure, 0.015 MPa; pH 5; feed concentration of complex metals, 50 ppm.

membranes were sintered at high temperatures. In particular, the K75D20 membrane sintered at 1250 °C did not catch metal ions except for Cu ions. It could be explained that Ca^{2+} and Mg^{2+} ions in dolomite reacted with mullite and became the anorthite and cordierite (eqs 7 and 8). According to some researchers,[9,37] using raw materials with big particles for membrane fabrication leads to the formation of integrated pores. These integrated pores lead to a decrease in both the specific surface area and liquid entry pressure of water, allowing some water with heavy-metal ions to pass through the membrane into the collection side. As a result, removal rates decline, revealing sharp increases in the permeate flux data.

The effect of the multielement concentration on the flux and removal rate is shown in Figure 17. The removal amount for all heavy-metal ions declined with an increase in the initial metal-ion concentration from 10 to 100 mg/L, and the flux for the filtration of the feed solution remained stable. These rate declines might be caused by the increase in the initial concentration, which leads to the saturation of the membrane sites. The number of available active sides on the membrane for the removal of metal ions decreased at a higher feed concentration. From this, the amount of metal ions removed depends on the initial concentration of metal ions.[38] On the other hand, it is a membrane, so the removal rate also depends on the pore size of the membrane, since, as mentioned above, integrated pores can allow some water together with metal ions to pass from the feed solution into the collection side.[37] Another factor is the presence of metal-ion competition during the removal process because it is a multielement system. Neris et al.[39] clarified the three types of metal-ion competition: it is

https://doi.org/10.1021/acsomega.4c06785
ACS Omega 2024, 9, 43068−43080

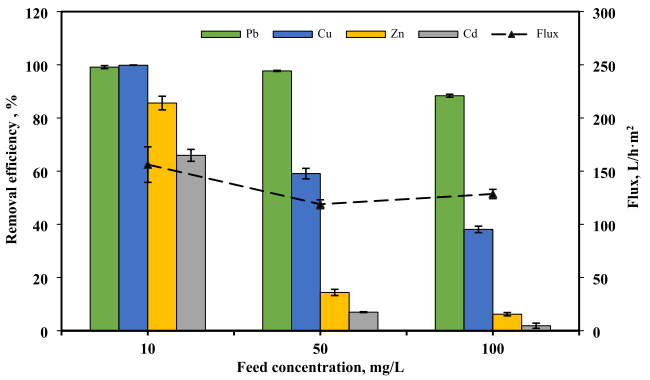

Figure 17. Effect of the feed concentration on the flux and removal rate of the K75D20 membrane sintered at 1100 °C for 4 h (applied pressure, 0.015 MPa; pH 5).

possible for metal-ion competition to increase or decrease, or metal ions may not interact in the multielement system. In our case, the removal rate followed the order Pb > Cu > Zn > Cd. The removal percent of Pb(II) was observed to be higher than that of other metal ions including Cu(II), Zn(II), and Cd(II). The Pb(II) ions were assigned to their ionic radius (1.19 Å) and Pauling electronegativity (2.33), which were higher than those of Cu(II) (0.73 and 1.95 Å), Zn(II) (0.83 and 1.63 Å), and Cd(II) ions (0.97 and 1.69 Å). High ionic radii and Pauling electronegativities involve stronger electrostatic interactions with active functional groups present in the membrane.[40]

In addition, we carried out element analysis using the K75D20 membrane sintered at 1100 °C for 4 h before and after removal for multiple heavy-metal ions. The results are illustrated in Figure 18. Before applying the membranes in the multielement system, Al, Si, Ca, Mg, and O were mainly found on the surface of the membrane. However, after applying the membranes in the multielement system, Al, Si, Ca, Mg, O, Pb, Cu, Zn, and Cd were detected on the membrane surface. This reveals that the membranes successfully caught the heavy-metal ions, which is also confirmed by XPS results (Figures 19 and 20). As illustrated in Figure 19, the Pb 4f, Cu 2p, Zn 2p, and Cd 3d signal peaks appear in the spectrum of the K75D20 (K75D20 + Pb, Cu, Zn, and Cd) membrane after removal of complex heavy metals, which indicates that heavy-metal ions adsorbed into the K75D20 membranes. In addition, each element's signal peaks are more clearly shown in Figure 20. Therefore, the mechanism of the metal-ion adsorption process into ceramic membranes can be explained by electrostatic attraction. The electrostatic reaction occurs between the negatively charged active sites of the membrane and the positively charged metal ions. The mechanism is as follows (eqs 10 and 11):[31]

$$2(\mathrm{SiO}^{-}) + \mathrm{M}^{2+} \rightarrow (\mathrm{Si\text{-}O})_2\mathrm{M} \quad (10)$$

$$2(\mathrm{AlO}^{-}) + \mathrm{M}^{2+} \rightarrow (\mathrm{Al\text{-}O})_2\mathrm{M} \quad (11)$$

Comparison with Other Membranes. The heavy-metal removal performance of K75D20 membranes compared with other reference's membranes is shown in Table 5. As shown in Table 5, it is clear that the K75D20 membranes have the potential to remove the heavy metals from aqueous media, and the obtained results are comparable with other membranes. Moreover, the K75D20 membranes showed higher water flux at low operating pressure compared to other membranes.

Membrane cost is a major concern for practical application on the industrial scale. The primary limiting factors of commercial ceramic membranes are the high cost of raw materials (pure oxides) and high sintering temperature. In this study, the usage of inexpensive precursors and low sintering temperature reduced the cost of raw materials and membrane production because dolomite is a cheaper material than kaolin.

CONCLUSIONS

In this work, kaolin- and dolomite-based adsorptive ceramic membranes (K95D0 and K65D30) were prepared for the removal of Pb(II), Cu(II), Zn(II), and Cd(II) from aqueous solutions. The dolomite addition of 20 wt %, sintering time of 4 h, and temperature of 1100 °C were found to be appropriate for membrane preparation. The dolomite addition improved both the compressive strength and pure water flux at a very low operating pressure (0.015 MPa). On the other hand, compared to commercially available alumina, titania, zirconia, and silicon carbide membranes, kaolin- and dolomite-based membranes have low mechanical strength, low temperature resistance, and high hygiene. But the obtained membrane with an optimal composition can be produced at a lower sintering temperature and raw material production cost compared to commercial ceramic membranes, which is one of its advantages for application. In addition, we have deeply clarified the adsorption

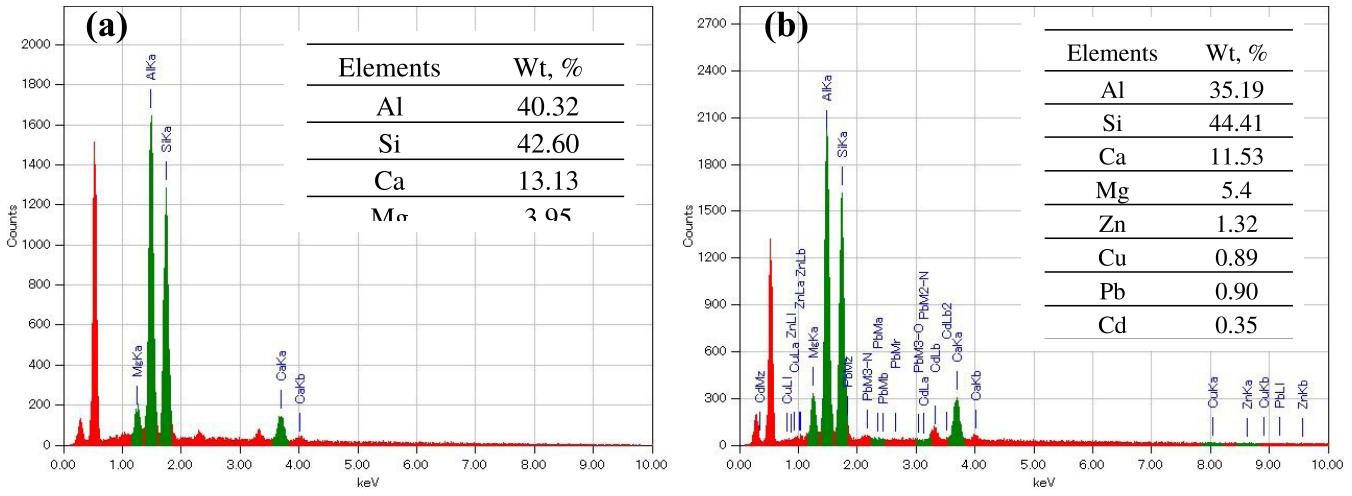

Figure 18. Elemental analysis of the K75D20 membrane sintered at 1100 °C for 4 h before (a) and after (b) the removal of complex heavy metals.

https://doi.org/10.1021/acsomega.4c06785
ACS Omega 2024, 9, 43068−43080

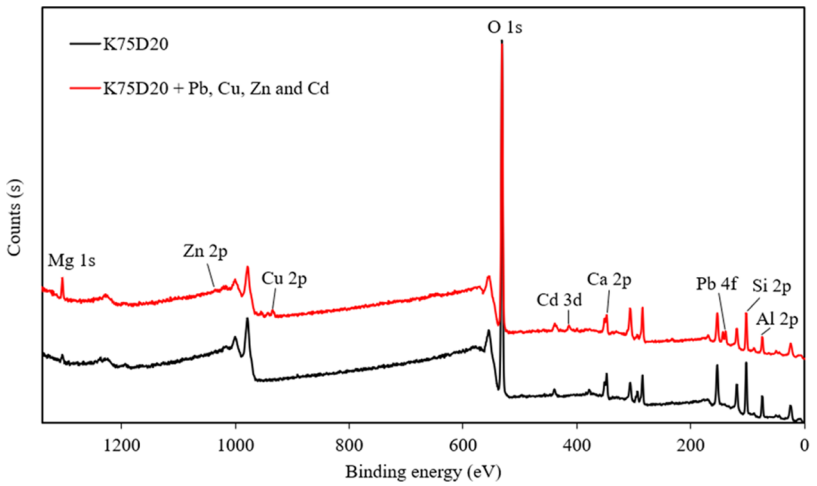

Figure 19. XPS patterns of the K75D20 membrane sintered at 1100 °C for 4 h before and after the removal of complex heavy metals.

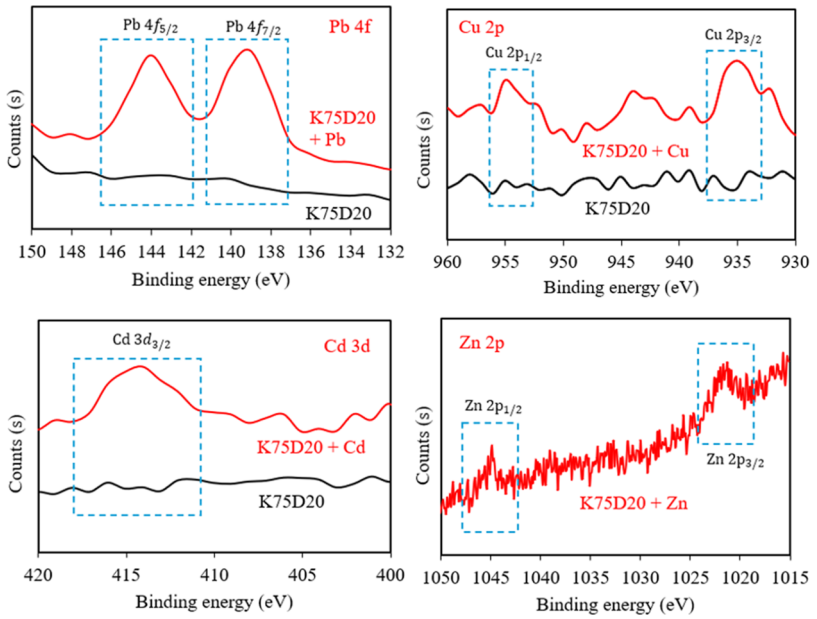

Figure 20. High-resolution XPS spectra of Pb 4f, Cu 2p, Cd 3d, and Zn 2p on the K75D20 membranes sintered at 1100 °C for 4 h before and after the removal of complex heavy metals.

Table 5. Comparison of Heavy-Metal Removal Performance on the Different Membranes

membranes	target pollutants	applied pressure (MPa)	flux (L/h·m^2)	feed pH	feed concentration (mg/L)	removal efficiency (%)	references
clay-based CM with SnO_2/MMT	Cu(II) and Zn(II)			<7	5−50	97.88−99.26 and 76.79−92.23	1
CHFM derived from RHA	Zn(II), and Pb(II)	0.2		5	50	99	41
GO/ATP composite	Cu(II), Pb(II) and Cd(II)	0.5	6.3	5	100	∼100	4
ZIF-300 MOF membrane	Cu(II)	0.1	39.2		460	99.21	42
kaolin-dolomite-based CM	Pb(II), Cu(II), Zn(II) and Cd(II)	0.015	118.89−156.15	5	10−100	88.3−99.1, 38.1−99.8, 6.2−85.6 and 1.8−65.9	this work

mechanism based on instrumental analysis from the viewpoints of both experimental and theoretical. The K75D20 membrane sintered at 1100 °C had the best removal rates for heavy-metal ions compared with the other membranes. The morphology, functional groups, charge distribution, and weakly bonded cations of the K75D20 membrane were highly influential in its ability to efficiently capture heavy-metal ions. The outcomes of this study offer beneficial perspectives on the role of membranes in heavy-metal removal and their possibilities for a broad range of applications, such as supports for membrane distillation, gas applications, and photocatalytic membranes.

https://doi.org/10.1021/acsomega.4c06785
ACS Omega 2024, 9, 43068−43080

AUTHOR INFORMATION

Corresponding Author

Naoki Kano − *Department of Chemistry and Chemical Engineering, Faculty of Engineering, Niigata University, Niigata 950-2181, Japan;* orcid.org/0000-0002-5590-2875; Phone: +81-025-262-7218; Email: kano@eng.niigata-u.ac.jp

Authors

Munkhpurev Bat-Amgalan − *Graduate School of Science and Technology, Niigata University, Niigata 950-2181, Japan; Department of Chemical Engineering, School of Applied Sciences, Mongolian University of Science and Technology, Ulaanbaatar 14191, Mongolia*

Naoto Miyamoto − *Department of Chemistry and Chemical Engineering, Faculty of Engineering, Niigata University, Niigata 950-2181, Japan*

Hee-Joon Kim − *Department of Chemistry and Chemical Engineering, Faculty of Engineering, Niigata University, Niigata 950-2181, Japan; Department of Environmental Chemistry and Chemical Engineering, School of Advanced Engineering, Kogakuin University, Hachioji 192-0015, Japan*

Ganchimeg Yunden − *Department of Chemical Engineering, School of Applied Sciences, Mongolian University of Science and Technology, Ulaanbaatar 14191, Mongolia*

Complete contact information is available at: https://pubs.acs.org/10.1021/acsomega.4c06785

Author Contributions

Methodology, experiment, data evaluation, and writing—original draft. M.B.-A.; instrument measurements. M.B.-A. and N.M.; supervision and writing—review and editing. N.K., H.-J.K., and G.Y. All authors have read and agreed to the published version of the manuscript.

Funding

This work was financially supported by a Grant-in-Aid for Scientific Research from the Japan Society for the Promotion of Science (Research Program (C), No. 21K12290).

Notes

The authors declare no competing financial interest.

ACKNOWLEDGMENTS

The authors thank Amaki, Y. of the Industrial Research Institute of Niigata Prefecture for the TG−DTA analyses and valuable advice. The authors are also grateful to Ohizumi, M. of the Office for Environment and Safety, and Dr. Watanabe, M.; Iwafune, K.; Nomoto, T.; Prof. Tanaka, T.; and Dr. Ohki, M. of the Facility of Engineering of Niigata University for permitting the use of ICP-AES, XRF, XRD, SEM-EDS, and the equipment for measuring mechanical strength.

REFERENCES

(1) Foorginezhad, S.; Zerafat, M. M.; Mohammadi, Y.; Asadnia, M. Fabrication of tubular ceramic membranes as low-cost adsorbent using natural clay for heavy metals removal. *Cleaner Eng. Technol.* **2022**, *10*, No. 100550.

(2) Cherono, F.; Mburu, N.; Kakoi, B. Adsorption of lead, copper and zinc in a multi-metal aqueous solution by waste rubber tires for the design of single batch adsorber. *Heliyon* **2021**, *7* (11), No. e08254.

(3) Sultana, M.; Rownok, M. H.; Sabrin, M.; Rahaman, M. H.; Alam, S. M. N. A review on experimental chemically modified activated carbon to enhance dye and heavy metals adsorption. *Cleaner Eng. Technol.* **2022**, *6*, No. 100382.

(4) Liu, W.; Wang, D.; Soomro, R. A.; Fu, F.; Qiao, N.; Yu, Y.; Wang, R.; Xu, B. Ceramic supported attapulgite-graphene oxide composite membrane for efficient removal of heavy metal contamination. *J. Membr. Sci.* **2019**, *591*, No. 117323.

(5) Chen, R.; Liao, X.; Ge, Q. A novel multinuclear zinc complex Zn-Bet-Tf2N for electroplating wastewater treatment using forward osmosis technique. *Chem. Eng. J.* **2021**, *404*, No. 126569.

(6) Carolin, C. F.; Kumar, P. S.; Saravanan, A.; Joshiba, G. J.; Naushad, M. Efficient techniques for the removal of toxic heavy metals from aquatic environment: A review. *J. Environ. Chem. Eng.* **2017**, *5* (3), 2782−2799.

(7) Saravanan, A.; Senthil Kumar, P.; Jeevanantham, S.; Karishma, S.; Tajsabreen, B.; Yaashikaa, P. R.; Reshma, B. Effective water/wastewater treatment methodologies for toxic pollutants removal: Processes and applications towards sustainable development. *Chemosphere* **2021**, *280*, No. 130595.

(8) Elanchezhiyan, S. S.; Karthikeyan, P.; Rathinam, K.; Hasmath Farzana, M.; Park, C. M. Magnetic kaolinite immobilized chitosan beads for the removal of Pb(II) and Cd(II) ions from an aqueous environment. *Carbohydr. Polym.* **2021**, *261*, No. 117892.

(9) Adam, M. R.; Salleh, N. M.; Othman, M. H. D.; Matsuura, T.; Ali, M. H.; Puteh, M. H.; Ismail, A. F.; Rahman, M. A.; Jaafar, J. The adsorptive removal of chromium (VI) in aqueous solution by novel natural zeolite based hollow fibre ceramic membrane. *J. Environ. Manage.* **2018**, *224*, 252−262.

(10) Hubadillah, S. K.; Jamalludin, M. R.; Othman, M. H. D.; Adam, M. R. A novel bio-ceramic hollow fibre membrane based hydroxyapatite derived from Tilapia fish bone for hybrid arsenic separation/adsorption from water. *Mater. Today: Proc.* **2023**, No. 232, DOI: 10.1016/j.matpr.2022.12.232.

(11) Samadi, A.; Gao, L.; Kong, L.; Orooji, Y.; Zhao, S. Waste-derived low-cost ceramic membranes for water treatment: Opportunities, challenges and future directions. *Resour., Conserv. Recycl.* **2022**, *185*, No. 106497.

(12) Huang, J.; Chen, H.; Zhou, T.; Qi, R.; Zhang, H. Alumina separation layer with uniform pore size applied on a support with broad pore size distribution. *Ceram. Int.* **2022**, *48* (21), 32513−32523.

(13) Malik, N.; Bulasara, V. K.; Basu, S. Preparation of novel porous ceramic microfiltration membranes from fly ash, kaolin and dolomite mixtures. *Ceram. Int.* **2020**, *46* (5), 6889−6898.

(14) Lakshmi Sandhya Rani, S.; Vinoth Kumar, R. Fabrication and characterization of ceramic membranes derived from inexpensive raw material fuller's earth clay. *Mater. Sci. Eng., B* **2022**, *284*, No. 115877.

(15) Kaur, H.; Bulasara, V. K.; Gupta, R. K. Effect of carbonates composition on the permeation characteristics of low-cost ceramic membrane supports. *J. Ind. Eng. Chem.* **2016**, *44*, 185−194.

(16) Omar, N. M. A.; Othman, M. H. D.; Tai, Z. S.; Puteh, M. H.; Jaafar, J.; Rahman, M. A.; Ismail, A. F.; Wong, K. Y. Effect of sintering temperature on functional properties of mullite-kaolinite and stainless steel composed hollow fibre membrane for oil-in-water emulsion separation. *J. Taiwan Inst. Chem. Eng.* **2023**, *146*, No. 104859.

(17) Huang, J.; Chen, H.; Qi, R.; Yang, J.; Li, Z.; Zhang, H. Porous ceramic membranes from coal fly ash with addition of various pore-forming agents for oil-in-water emulsion separation. *J. Environ. Chem. Eng.* **2023**, *11* (3), No. 109929.

(18) Saja, S.; Bouazizi, A.; Achiou, B.; Ouaddari, H.; Karim, A.; Ouammou, M.; Aaddane, A.; Bennazha, J.; Alami Younssi, S. Fabrication of low-cost ceramic ultrafiltration membrane made from bentonite clay and its application for soluble dyes removal. *J. Eur. Ceram. Soc.* **2020**, *40* (6), 2453−2462.

(19) Guesmi, Y.; Lafi, R.; Agougui, H.; Jabli, M.; Oun, A.; Majumdar, S.; Hafiane, A. Synthesis and characterization of alpha alumina-natural apatite based porous ceramic support for filtration application. *Mater. Chem. Phys.* **2020**, *239*, No. 122067.

(20) Hubadillah, S. K.; Jamalludin, M. R.; Dzarfan Othman, M. H.; Iwamoto, Y. Recent progress on low-cost ceramic membrane for water and wastewater treatment. *Ceram. Int.* **2022**, *48* (17), 24157−24191.

(21) Twibi, M. F.; Othman, M. H. D.; Hubadillah, S. K.; Alftessi, S. A.; Adam, M. R. B.; Ismail, A. F.; Rahman, M. A.; Jaafar, J.; Raji, Y. O.; Abd

Aziz, M. H.; et al. Hydrophobic mullite ceramic hollow fibre membrane (Hy-MHFM) for seawater desalination via direct contact membrane distillation (DCMD). *J. Eur. Ceram. Soc.* **2021**, *41* (13), 6578−6585.
(22) Bessa, L. P.; Terra, N. M.; Cardoso, V. L.; Reis, M. H. M. Macroporous dolomite hollow fibers sintered at different temperatures toward widened applications. *Ceram. Int.* **2017**, *43* (18), 16283−16291.
(23) Khoshraftar, Z.; Masoumi, H.; Ghaemi, A. An insight into the potential of dolomite powder as a sorbent in the elimination of heavy metals: A review. *Case Stud. Chem. Environ. Eng.* **2023**, *7*, No. 100276.
(24) Liu, J.; Dong, Y.; Dong, X.; Hampshire, S.; Zhu, L.; Zhu, Z.; Li, L. Feasible recycling of industrial waste coal fly ash for preparation of anorthite-cordierite based porous ceramic membrane supports with addition of dolomite. *J. Eur. Ceram. Soc.* **2016**, *36* (4), 1059−1071.
(25) Adam, M. R.; Hubadillah, S. K.; Aziz, M. H. A.; Jamalludin, M. R. The emergence of adsorptive membrane treatment for pollutants removal—A mini bibliometric analysis study. *Mater. Today: Proc.* **2023**, *88*, 15−22.
(26) Yin, N.; Wang, K.; Wang, L.; Li, Z. Amino-functionalized MOFs combining ceramic membrane ultrafiltration for Pb (II) removal. *Chem. Eng. J.* **2016**, *306*, 619−628.
(27) Ainscough, T. J.; Alagappan, P.; Oatley-Radcliffe, D. L.; Barron, A. R. A hybrid super hydrophilic ceramic membrane and carbon nanotube adsorption process for clean water production and heavy metal removal and recovery in remote locations. *J. Water Process Eng.* **2017**, *19*, 220−230.
(28) Chee, D. N. A.; Aziz, F.; Ismail, A. F.; Kueh, A. B. H.; Amin, M. A. M.; Amran, M. Adsorptive zeolitic imidazolate framework-8 membrane on ceramic support for the removal of lead(II) ions. *Chem. Eng. Sci.* **2023**, *276*, No. 118775.
(29) Zhang, P.; Gong, J.-L.; Zeng, G.-M.; Deng, C.-H.; Yang, H.-C.; Liu, H.-Y.; Huan, S.-Y. Cross-linking to prepare composite graphene oxide-framework membranes with high-flux for dyes and heavy metal ions removal. *Chem. Eng. J.* **2017**, *322*, 657−666.
(30) Zhang, X.; Guo, Y. X.; Ren, B.; Zhao, N.; Hu, Y. C.; Wang, X. Preparation of graphene oxide membranes by vacuum self-assembly for copper separation in water. *Diamond Relat. Mater.* **2021**, *120*, No. 108687.
(31) Mahatmanti, F. W.; Jumaeri, J.; Kusumastuti, E. The adsorption behavior of individual Cu(II), Zn(II), and Cd(II) ions over a CuO-modified ceramic membrane synthesized from fly ash. *J. King Saud Univ., Sci.* **2023**, *35* (8), No. 102866.
(32) Shoshaa, R.; Ashfaq, M. Y.; Al-Ghouti, M. A. Recent developments in ultrafiltration membrane technology for the removal of potentially toxic elements, and enhanced antifouling performance: A review. *Environ. Technol. Innov.* **2023**, *31*, No. 103162.
(33) Nasir, A. M.; Goh, P. S.; Abdullah, M. S.; Ng, B. C.; Ismail, A. F. Adsorptive nanocomposite membranes for heavy metal remediation: Recent progresses and challenges. *Chemosphere* **2019**, *232*, 96−112.
(34) Bat-Amgalan, M.; Miyamoto, N.; Kano, N.; Yunden, G.; Kim, H.-J. Preparation and Characterization of Low-Cost Ceramic Membrane Coated with Chitosan: Application to the Ultrafine Filtration of Cr(VI). *Membranes* **2022**, *12* (9), 835.
(35) Wang, S.; Gainey, L.; Wang, X.; Mackinnon, I. D. R.; Xi, Y. Influence of palygorskite on in-situ thermal behaviours of clay mixtures and properties of fired bricks. *Appl. Clay Sci.* **2022**, *216*, No. 106384.
(36) Khoshraftar, Z.; Masoumi, H.; Ghaemi, A. Experimental, response surface methodology (RSM) and mass transfer modeling of heavy metals elimination using dolomite powder as an economical adsorbent. *Case Stud. Chem. Environ. Eng.* **2023**, *7*, No. 100329.
(37) Hubadillah, S. K.; Othman, M. H. D.; Ismail, A. F.; Rahman, M. A.; Jaafar, J. A low cost hydrophobic kaolin hollow fiber membrane (h-KHFM) for arsenic removal from aqueous solution via direct contact membrane distillation. *Sep. Purif. Technol.* **2019**, *214*, 31−39.
(38) Abdel Salam, O. E.; Reiad, N. A.; ElShafei, M. M. A study of the removal characteristics of heavy metals from wastewater by low-cost adsorbents. *J. Adv. Res.* **2011**, *2* (4), 297−303.
(39) Neris, J. B.; Luzardo, F. H. M.; da Silva, E. G. P.; Velasco, F. G. Evaluation of adsorption processes of metal ions in multi-element aqueous systems by lignocellulosic adsorbents applying different isotherms: A critical review. *Chem. Eng. J.* **2019**, *357*, 404−420.
(40) Soetaredjo, F. E.; Kurniawan, A.; Ki, O. L.; Ismadji, S. Incorporation of selectivity factor in modeling binary component adsorption isotherms for heavy metals-biomass system. *Chem. Eng. J.* **2013**, *219*, 137−148.
(41) Hubadillah, S. K.; Othman, M. H. D.; Harun, Z.; Ismail, A. F.; Rahman, M. A.; Jaafar, J. A novel green ceramic hollow fiber membrane (CHFM) derived from rice husk ash as combined adsorbent-separator for efficient heavy metals removal. *Ceram. Int.* **2017**, *43* (5), 4716−4720.
(42) Yuan, J.; Hung, W.-S.; Zhu, H.; Guan, K.; Ji, Y.; Mao, Y.; Liu, G.; Lee, K.-R.; Jin, W. Fabrication of ZIF-300 membrane and its application for efficient removal of heavy metal ions from wastewater. *J. Membr. Sci.* **2019**, *572*, 20−27.

https://doi.org/10.1021/acsomega.4c06785
ACS Omega 2024, 9, 43068−43080